

## Molecular Structures of Thimerosal (Merthiolate) and Other Arylthiolate Mercury Alkyl Compounds

Jonathan G. Melnick, Kevin Yurkerwich, Daniela Buccella, Wesley Sattler, and Gerard Parkin\*

Department of Chemistry, Columbia University, New York, New York 10027

Received March 26, 2008

The molecular structure of sodium ethylmercury thiosalicylate (also known as thimerosal and Merthiolate) and related arylthiolate mercury alkyl compounds, namely PhSHgMe and PhSHgEt, have been determined by single crystal X-ray diffraction.  $^1\text{H}$  NMR spectroscopic studies indicate that the appearance of the  $^{199}\text{Hg}$  mercury satellites of the ethyl group of thimerosal is highly dependent on the magnetic field and the viscosity of the solvent as a consequence of relaxation due to chemical shift anisotropy.

## Introduction

Sodium ethylmercury thiosalicylate,  $[(\text{Ar}^{\text{CO}_2})\text{SHgEt}]\text{Na}$ , commonly known as thimerosal (Figure 1),<sup>1,2</sup> is a controversial vaccine preservative with proposed links to autism in children, although the connection is being intensely debated.<sup>3,4</sup> Thimerosal was first introduced as a pharmaceutical ingredient in the early 1930s under the trade name Merthiolate<sup>5</sup> and found popular use for the topical treatment of cuts and wounds.<sup>6</sup> In addition to its use as a vaccine preservative and as an antiseptic, other applications of thimerosal that result from its antimicrobial properties include: contact lens cleaners; soap-free cleansers; cosmetics; eye, nose and ear drops; and skin test antigens.<sup>1,7</sup> Considering the widespread applications of thimerosal, and the fact that

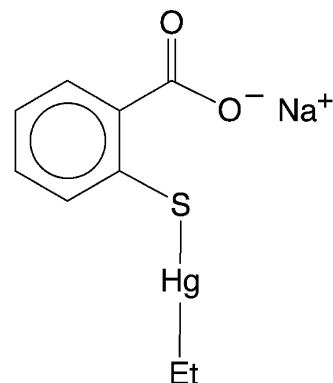


Figure 1. Thimerosal.

many mercury compounds constitute a health risk,<sup>8</sup> it is surprising that the chemistry of this molecule is virtually unknown<sup>9</sup> and that its 3-dimensional structure has not been determined. Therefore, we report herein the molecular structures of thimerosal and related arylthiolate mercury alkyl compounds, namely PhSHgMe and PhSHgEt, as determined by X-ray diffraction.

## Results and Discussion

**Structural and Spectroscopic Characterization of Thimerosal.** Although thimerosal was first reported in 1928<sup>10–12</sup> and subsequently found many applications, there

\* To whom correspondence should be addressed. E-mail: parkin@columbia.edu.

- (1) Geier, D. A.; Sykes, L. K.; Geier, M. R. *J. Toxicol. Environ. Health, Part B* **2007**, *10*, 575–596.
- (2) In addition to the trade name Merthiolate, there are many other synonyms for thimerosal, some of which include: thiomersal, eliclide, estivin, mercurothiolate, merfamin, merphol, merseptyl, mertorgan, merzonin, and nosemack.
- (3) (a) Blaxill, M. F.; Redwood, L.; Bernard, S. *Med. Hypotheses* **2004**, *62*, 788–794. (b) Geier, D. A.; Geier, M. R. *J. Toxicol. Environ. Health, Part A* **2007**, *70*, 837–851. (c) Baker, J. P. *Am. J. Public Health* **2008**, *98*, 2–11.
- (4) (a) Bernard, S. *New Eng. J. Med.* **2008**, *358*, 93. (b) Rooney, J. P. K. *New Eng. J. Med.* **2008**, *358*, 93–94. (c) Thompson, W. W.; Price, C.; DeStafano, F. *New Eng. J. Med.* **2008**, *358*, 94.
- (5) Powell, H. M.; Jamieson, W. A. *Am. J. Hygiene* **1931**, *13*, 296–310.
- (6) Ohno, H.; Doi, R.; Kashima, Y.; Murae, S.; Kizaki, T.; Hitomi, Y.; Nakano, N.; Harada, M. *Bull. Environ. Contam. Toxicol.* **2004**, *73*, 777–780.
- (7) (a) Gil, S.; Lavilla, I.; Bendicho, C. *J. Anal. At. Spectrom.* **2007**, *22*, 569–572. (b) Fagundes, A.; Marzochi, M. C. A.; Perez, M.; Schubach, A.; Ferreira, A.; Silva, J. P.; Schubach, T.; Marzochi, K. B. F. *Acta Trop.* **2007**, *101*, 25–30. (c) Meyer, B. K.; Ni, A.; Hu, B.; Shi, L. *J. Pharm. Sci.* **2007**, *96*, 3155–3167.

(8) Clarkson, T. W.; Magos, L. *Crit. Rev. Toxicol.* **2006**, *36*, 609–662.

(9) For two brief reports pertaining to the chemistry of thimerosal, see: (a) Trikojus, V. M. *Nature* **1946**, *158*, 472–473. (b) Tan, M.; Parkin, J. E. *Int. J. Pharm.* **2000**, *208*, 23–34.

(10) Kharasch, M. S. U.S. Patent 1,672,615, 1928.

(11) For a later synthesis, see: (a) Swirski, A.; Kotler-Brajtburg, J.; Dahlig, W.; Pasynkiewicz, S. *Przem. Chem.* **1960**, *39*, 371–372.

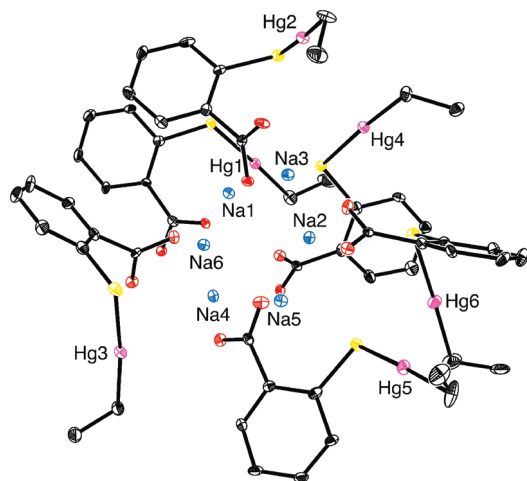


Figure 2. Asymmetric unit of thimerosal.

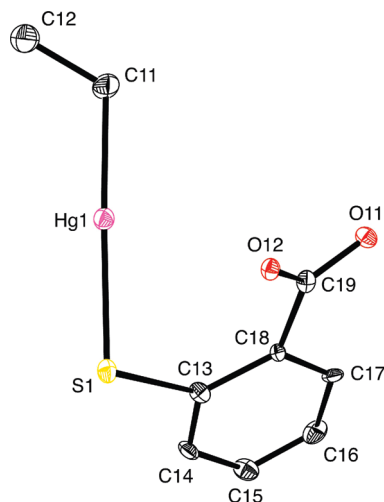


Figure 3. Molecular structure of one of the anions of thimerosal in the asymmetric unit.

are almost no reported details pertaining to its structure, spectroscopic properties and reactivity. For this reason, we deemed it appropriate to determine the molecular structure of thimerosal by X-ray diffraction.

The crystal structure of thimerosal (obtained from methanol), as illustrated in Figures 2 and 3, is composed of a complex network consisting of  $[(\text{ArCO}_2)\text{SHgEt}]^-$  anions connected to  $\text{Na}^+$  cations via both the oxygen and sulfur atoms of the thiosalicylate ligand. The asymmetric unit consists of six formula units of  $\{[(\text{ArCO}_2)\text{SHgEt}]\text{Na}\}$  that differ in subtle ways. For example, some of the sodium ions coordinate only to the carboxylate oxygen atoms, while other sodium ions also coordinate to the sulfur atom. With respect to the  $[(\text{ArCO}_2)\text{SHgEt}]^-$  moieties, the principal differences are associated with the torsion angles involving the  $(\text{ArCO}_2)$  group, such that the  $\text{Hg}\cdots\text{O}$  distances within each unit range from 2.71 Å to 4.91 Å. Other than the torsion angles, the structures of  $[(\text{ArCO}_2)\text{SHgEt}]^-$  are similar, with each mercury having the linear two-coordinate geometry that is common

**Table 1.** Comparison of Bond Length (Å) and Bond Angle (deg) Data for the Six Independent Molecules of  $[(\text{ArCO}_2)\text{SHgEt}]\text{Na}$  in the Asymmetric Unit

	$d(\text{Hg}-\text{C})/\text{Å}$	$d(\text{Hg}-\text{S})/\text{Å}$	$\text{C}-\text{Hg}-\text{S}/\text{deg}$
molecule #1	2.075(13)	2.383(3)	178.0(4)
molecule #2	2.081(13)	2.364(3)	176.9(4)
molecule #3	2.129(12)	2.391(3)	173.3(4)
molecule #4	2.094(11)	2.376(3)	176.5(4)
molecule #5	2.100(12)	2.371(3)	175.0(5)
molecule #6	2.075(16)	2.363(3)	176.8(7)

**Table 2.** Comparison of Average Bond Length (Å) and Bond Angle (deg) Data for  $\text{ArSHgEt}$

	$d(\text{Hg}-\text{C})/\text{Å}$	$d(\text{Hg}-\text{S})/\text{Å}$	$\text{C}-\text{Hg}-\text{S}/\text{deg}$
$[(\text{ArCO}_2)\text{SHgEt}]\text{Na}$	2.07(1)	2.383(3)	178.0(4)
$\text{PhSHgEt}$	2.07(1)	2.369(2)	178.1(3)

for alkyl and thiolate compounds.<sup>13–16</sup> Selected bond lengths and angles for the  $[(\text{ArCO}_2)\text{SHgEt}]^-$  moieties are summarized in Table 1, with the average values listed in Table 2.

In view of the unusual hexameric composition of the asymmetric unit, it was important to establish whether the derived structure of the crystal studied is representative of the bulk material. Evidence that the crystal is indeed representative of the bulk was provided by the favorable comparison of the experimental X-ray powder diffraction pattern (Mo radiation) with that predicted on the basis of the atomic coordinates and unit cell parameters; furthermore, the powder pattern predicted for Cu radiation (Figure 4) corresponds closely to the experimental data reported elsewhere.<sup>17</sup>

<sup>199</sup>Hg NMR spectroscopic studies are in accord with thimerosal also possessing a linear two-coordinate geometry in solution. Specifically, the <sup>199</sup>Hg NMR chemical shift of thimerosal is −784 ppm, which is within the range observed for two-coordinate mercury thiolate compounds.<sup>18,19</sup> The signal is a well-resolved triplet of quartets, corresponding to <sup>2</sup>*J*<sub>Hg–H</sub> and <sup>3</sup>*J*<sub>Hg–H</sub> coupling to the hydrogen atoms of the ethyl group (Figure 5). Correspondingly, the <sup>1</sup>H and <sup>13</sup>C NMR spectra exhibit <sup>199</sup>Hg satellites (16.9% abundance), as illustrated in Figures 6 and 7. *J*<sub>Hg–C</sub> and *J*<sub>Hg–H</sub> coupling constant data are listed in Table 3. Of particular note, while

- (13) (a) Casa, J. S.; García-Tasende, M. S.; Sordo, J. *Coord. Chem. Rev.* **1999**, 193–195, 283–359. (b) Holloway, C. E.; Melnik, M. J. *Organomet. Chem.* **1995**, 495, 1–31. (c) Rabenstein, D. L. *Acc. Chem. Res.* **1978**, 11, 100–107.
- (14) Wright, J. G.; Natan, M. J.; MacDonnell, F. M.; Ralston, D. M.; O'Halloran, T. V. *Prog. Inorg. Chem.* **1990**, 38, 323–412.
- (15) The propensity of mercury to adopt linear coordination is often attributed to relativistic effects which stabilize the 6s orbital, thereby resulting in a large 6s–6p energy gap which limits the use of the 6p orbitals, and to a small 5d–6s energy gap that favors linear *sd*<sub>z</sub><sup>2</sup> hybridization. Other factors have also, nevertheless, been considered. See, for example: (a) Pyykkö, P.; Desclaux, J.-P. *Acc. Chem. Res.* **1979**, 12, 276–281. (b) Pyykkö, P. *Chem. Rev.* **1988**, 88, 563–594. (c) Kaupp, M.; von Schnering, H. G. *Inorg. Chem.* **1994**, 33, 2555–2564. (d) Tossell, J. A.; Vaughan, D. J. *Inorg. Chem.* **1981**, 20, 3333–3340.
- (16) As observed for many linear mercury complexes, in addition to the primary interactions, the mercury centers exhibit longer range secondary interactions to the thiolate sulfur atoms of adjacent molecules.
- (17) Koundourellis, J. E.; Malliou, E. T.; Sullivan, R. A. L.; Chapman, B. J. *Chem. Eng. Data* **2000**, 45, 1001–1006.
- (18) Wright, J. G.; Natan, M. J.; MacDonnell, F. M.; Ralston, D. M.; O'Halloran, T. V. *Prog. Inorg. Chem.* **1990**, 38, 323–412.
- (19) (a) Almagro, X.; Clegg, W.; Cucurull-Sánchez, L.; González-Duarte, P.; Travería, M. J. *Organomet. Chem.* **2001**, 623, 137–148. (b) Carlton, L.; White, D. *Polyhedron* **1990**, 9, 2717–2720.

(12) The name “thimerosal” for sodium ethylmercury thiosalicylate appeared in the literature much later. For an early use of the name “thimerosal”, see: Hughes, E. J. *Drug Stand.* **1952**, 20, 121–124.

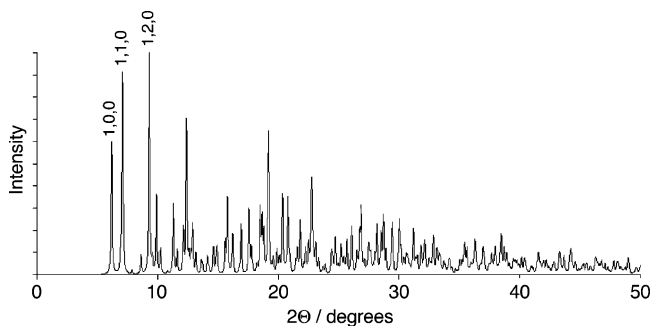


**Figure 4.** Calculated powder pattern for thimerosal on the basis of the experimental unit cell data (Cu radiation).

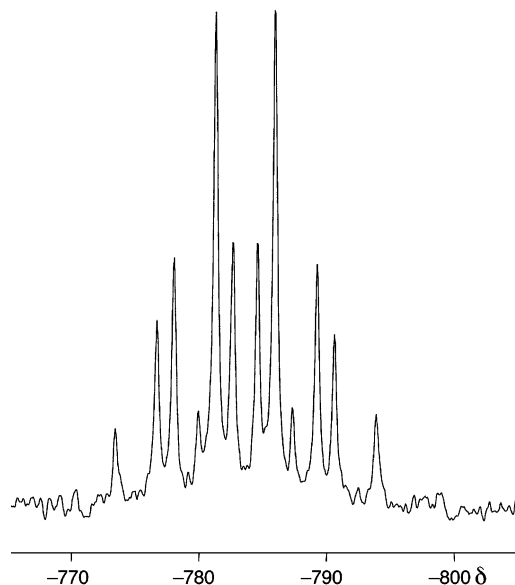


**Figure 5.**  $^{199}\text{Hg}$  NMR spectrum (53.75 MHz) of thimerosal in  $\text{D}_2\text{O}$ .

$^1J_{\text{Hg}-\text{C}}$  (1316 Hz) is considerably larger than  $^2J_{\text{Hg}-\text{C}}$  (74 Hz),  $^2J_{\text{Hg}-\text{H}}$  (176 Hz) is significantly smaller than  $^3J_{\text{Hg}-\text{H}}$  (250 Hz). A similar trend in  $^2J_{\text{Hg}-\text{H}}$  and  $^3J_{\text{Hg}-\text{H}}$  coupling constants is also observed for other  $\text{EtHgX}$  derivatives.<sup>20</sup>

Other interesting aspects of the  $^1\text{H}$  NMR spectrum of thimerosal pertain to the chemical shifts of the  $\text{CH}_2$  and  $\text{CH}_3$  groups and the nature of the  $^{199}\text{Hg}$  satellites. With respect to the chemical shifts, it is noteworthy that the  $^1\text{H}$  NMR chemical shift of the  $\text{CH}_2$  group is *downfield* of the  $\text{CH}_3$  group (Figure 7), an order that is opposite to that for other  $\text{EtHgX}$  derivatives ( $\text{X} = \text{CN}, \text{Br}, \text{Cl}, \text{NO}_3, \text{I}, \text{ClO}_4$ ), with the exception of  $\text{Et}_2\text{Hg}$ .<sup>20</sup>

The feature of interest pertaining to the  $^{199}\text{Hg}$  satellites of the  $^1\text{H}$  NMR spectrum is concerned with the fact that, whereas the main signals associated with the ethyl group consist of a well defined triplet and quartet, the satellites are broad such that  $^3J_{\text{H}-\text{H}}$  is not well resolved. Furthermore, the appearance of the  $^{199}\text{Hg}$  satellites are dependent on the magnetic field, with the ability to resolve  $^3J_{\text{H}-\text{H}}$  coupling in the satellites decreasing with increasing magnetic field strength (Figure 7). The origin of the magnetic field dependence of the satellites is due to relaxation by chemical

shift anisotropy,<sup>21</sup> a mechanism that not only applies to  $^{199}\text{Hg}$ ,<sup>22</sup> but other nuclei such as  $^{31}\text{P}$ ,<sup>23</sup>  $^{77}\text{Se}$ ,<sup>23b,24</sup>  $^{57}\text{Fe}$ ,<sup>25</sup>  $^{103}\text{Rh}$ ,<sup>26</sup>  $^{195}\text{Pt}$ ,<sup>27</sup>  $^{207}\text{Pb}$ ,<sup>28</sup> and  $^{205}\text{Tl}$ .<sup>29,30</sup> Specifically, for situations in which the condition  $\omega_0\tau_c \ll 1$  is satisfied, the relaxation component due to chemical shift anisotropy is directly proportional to  $B_0^2$ .<sup>21</sup> Thus, as the strength of the magnetic field increases,  $w_{1/2}$  of the satellites increases such that it is not possible to resolve the  $^3J_{\text{H}-\text{H}}$  coupling.

Since relaxation via chemical shift anisotropy is influenced by the rotational correlation time ( $\tau_c$ ), the line width of the satellites is a function of the viscosity of the solvent. Specifically, for  $\omega_0\tau_c \ll 1$ , relaxation due to chemical shift anisotropy is proportional to the rotational correlation time ( $\tau_c$ ) which is dependent on the viscosity.<sup>21</sup> For this reason, the multiplet structure of the mercury satellites of the ethyl group of thimerosal are much better resolved in methanol (Figure 8) and acetone that have a lower viscosity than that of water.<sup>31</sup>

**Structural Characterization of  $\text{PhSHgMe}$  and  $\text{PhSHgEt}$ .** Interestingly, while arylthiolate mercury complexes of the type  $\text{ArSHgR}$  are known,<sup>19,32</sup> structurally characterized examples listed in the Cambridge Structural Database<sup>33</sup> are restricted to methyl and phenyl derivatives. As such, we considered it worthwhile to determine the

- (21) (a) Farrar, T. C.; Becker, E. D. *Pulse and FT NMR*; Academic Press: New York, 1971. (b) Farrar, T. C. *Introduction to Pulse NMR Spectroscopy*; The Farragut Press: Chicago, Madison, 1989. (c) Thouvenot, R. *L'Actualité Chimique* **1996**, 7, 102–111. (d) Kowalewski, J.; Mäler, L. *Nuclear Spin Relaxation in Liquids: Theory, Experiments, and Applications*; Taylor and Francis: New York, 2006.
- (22) (a) Benn, R.; Günther, H.; Maercker, A.; Menger, V.; Schmitt, P. *Angew. Chem., Int. Ed. Engl.* **1982**, 21, 295–296. (b) Gillies, D. G.; Blaauw, L. P.; Hays, G. R.; Huis, R.; Clague, A. D. H. *J. Magn. Reson.* **1981**, 42, 420–428. (c) Cecconi, F.; Ghilardi, C. A.; Innocenti, P.; Midollini, S.; Orlandini, A.; Ienco, A.; Vacca, A. *J. Chem. Soc., Dalton Trans.* **1996**, 2821–2826.
- (23) (a) Randall, L. H.; Carty, A. J. *Inorg. Chem.* **1989**, 28, 1194–1196. (b) Penner, G. H. *Can. J. Chem.* **1991**, 69, 1054–1056.
- (24) Wong, T. C.; Ang, T. T.; Guziec, F. S., Jr.; Moustakis, C. A. *J. Magn. Reson.* **1984**, 57, 463–470.
- (25) Baltzer, L.; Becker, E. D.; Averill, B. A.; Hutchinson, J. M.; Gansow, O. A. *J. Am. Chem. Soc.* **1984**, 106, 2444–2446.
- (26) (a) Socol, S. M.; Meek, D. W. *Inorg. Chim. Acta* **1985**, 101, L45–L46. (b) Cocivera, M.; Ferguson, G.; Lenkinski, R. E.; Szczecinski, P.; Lalor, F. J.; O'Sullivan, D. J. *J. Magn. Reson.* **1982**, 46, 168–171.
- (27) (a) Lallemand, J.-Y.; Soulié, J.; Chottard, J.-C. *J. Chem. Soc., Chem. Commun.* **1980**, 436–438. (b) Anklin, C. G.; Pregosin, P. S. *Magn. Reson. Chem.* **1985**, 23, 671–675. (c) Benn, R.; Büch, H. M.; Reinhardt, R.-D. *Magn. Reson. Chem.* **1985**, 23, 559–564. (d) Dechter, J. J.; Kowaleski, J. *J. Magn. Reson.* **1984**, 59, 146–149. (e) Pregosin, P. S. *Coord. Chem. Rev.* **1982**, 44, 247–291. (f) Ismail, I. M.; Kerrison, S. J. S.; Sadler, P. J. *Polyhedron* **1982**, 1, 57–59. (g) Skvortsov, A. N. *Russ. J. Gen. Chem.* **2000**, 70, 1023–1027. (h) Hughes, R. P.; Sweetser, J. T.; Tawa, M. D.; Williamson, A.; Incarvito, C. D.; Rhatigan, B.; Rheingold, A. L.; Rossi, G. *Organometallics* **2001**, 20, 3800–3810. (i) Reinartz, S.; Baik, M.-H.; White, P. S.; Brookhart, M.; Templeton, J. L. *Inorg. Chem.* **2001**, 40, 4726–4732. (j) Reinartz, S.; White, P. S.; Brookhart, M.; Templeton, J. L. *Organometallics* **2000**, 19, 3854–3866.
- (28) (a) Hawk, R. M.; Sharp, P. R. *J. Chem. Phys.* **1974**, 60, 1522–1527. (b) Hays, G. R.; Gillies, D. G.; Blaauw, L. P.; Clague, A. D. H. *J. Magn. Reson.* **1981**, 45, 102–107.
- (29) (a) Brady, F.; Matthews, R. W.; Forster, M. J.; Gillies, D. G. *Inorg. Nucl. Chem. Lett.* **1981**, 17, 155–159. (b) Hinton, J. F.; Ladner, K. H. *J. Magn. Reson.* **1978**, 32, 303–306. (c) Brady, F.; Matthews, R. W.; Forster, M. J.; Gillies, D. G. *J. Chem. Soc., Chem. Commun.* **1981**, 911–912. (d) Ghosh, P.; Desrosiers, P. J.; Parkin, G. *J. Am. Chem. Soc.* **1998**, 120, 10416–10422.
- (30) Benn, R.; Rufinska, A. *Angew. Chem., Int. Ed. Engl.* **1986**, 25, 861–881.

(20) Petrosya, V. S.; Reutov, O. A. *J. Organomet. Chem.* **1974**, 76, 123–169.

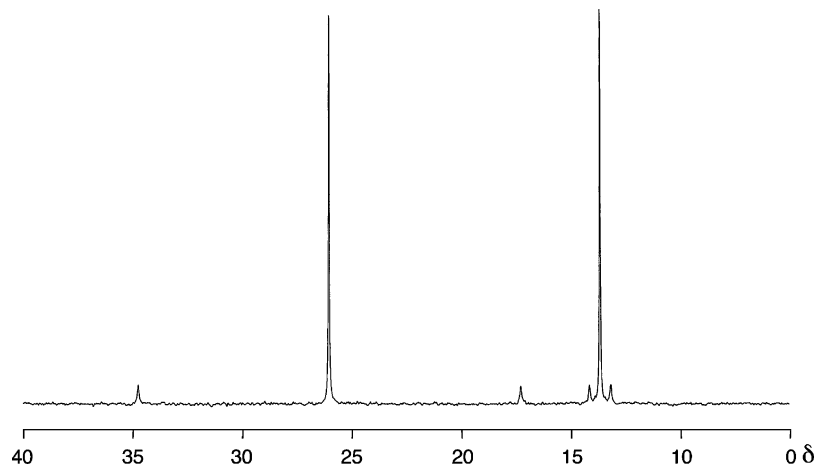


Figure 6.  $^{13}\text{C}\{^1\text{H}\}$  NMR spectrum (75.4677 MHz) of thimerosal in  $\text{D}_2\text{O}$ .

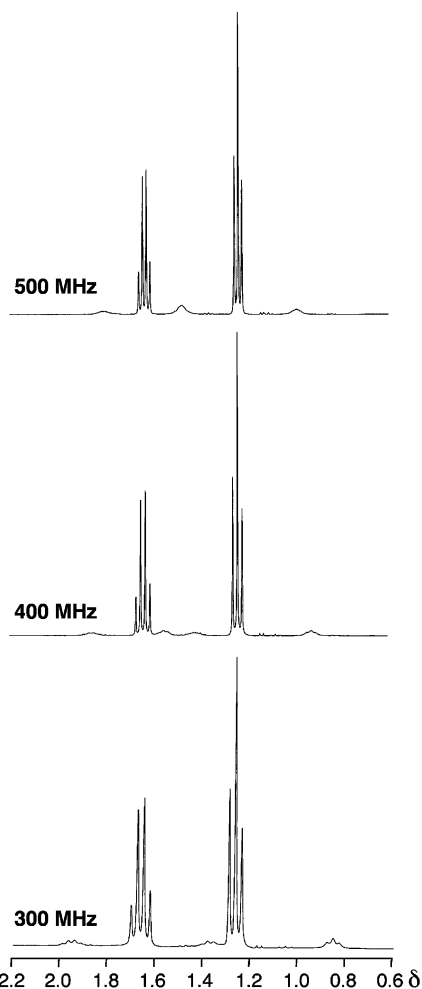


Figure 7.  $^1\text{H}$  NMR spectra of Thimerosal in  $\text{D}_2\text{O}$  as a function of the magnetic field strength.

Table 3.  $^1\text{H}$  and  $^{13}\text{C}$  NMR Spectroscopic Data for the Ethyl Ligand of Thimerosal in  $\text{D}_2\text{O}$

$^1\text{H}$	$^{13}\text{C}$
$\delta(\text{CH}_2) = 1.65$	$\delta(\text{CH}_2) = 28.3$
$^3J_{\text{H-H}} = 8$ ; $^2J_{\text{Hg-H}} = 176$	$^1J_{\text{C-H}} = 136$ ; $^1J_{\text{Hg-C}} = 1316$
$\delta(\text{CH}_3) = 1.26$	$\delta(\text{CH}_3) = 15.9$
$^3J_{\text{H-H}} = 8$ ; $^3J_{\text{Hg-H}} = 250$	$^1J_{\text{C-H}} = 126$ ; $^2J_{\text{Hg-C}} = 74$

molecular structure of the ethyl complex  $\text{PhSHgEt}^{34,35}$  to evaluate whether the anionic substituent on the phenyl group

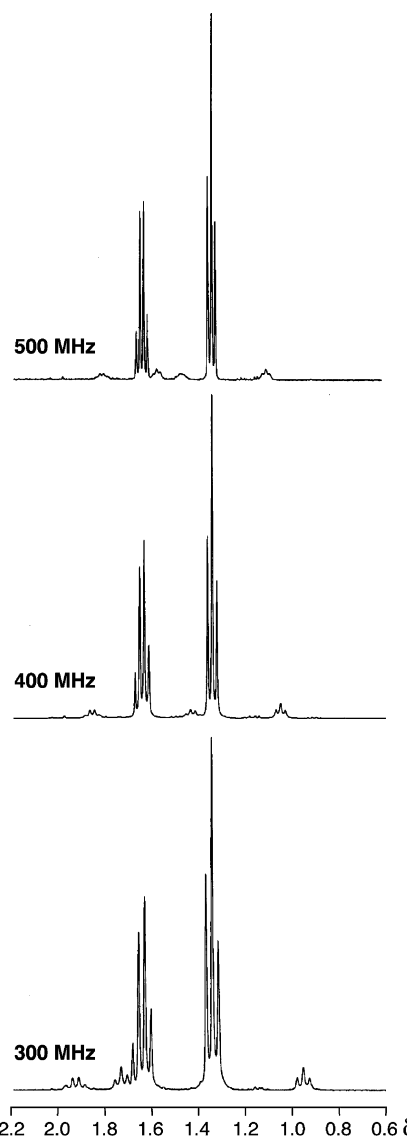
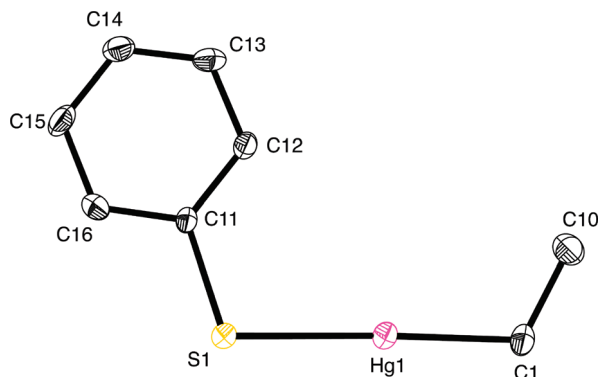


Figure 8.  $^1\text{H}$  NMR spectra of thimerosal in  $\text{CD}_3\text{OD}$  as a function of the magnetic field strength.

exerts any influence on the coordination geometry of the mercury center. The molecular structure of  $\text{PhSHgEt}$ , as determined by X-ray diffraction, is illustrated in Figure 9, while selected metrical data are summarized in Table 2.





**Figure 9.** Molecular structure of one of the crystallographically independent molecules of PhHgEt in the asymmetric unit.

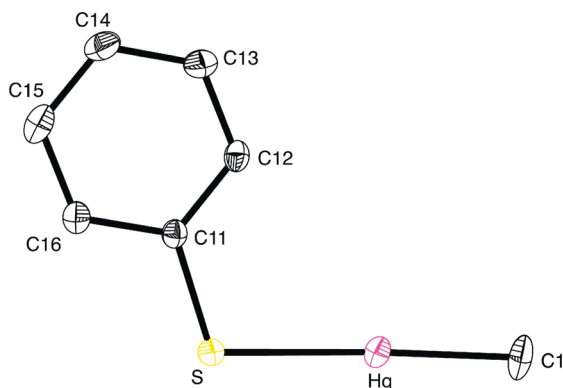


**Figure 10.** Molecular structure of PhSHgMe.

**Table 4.** Comparison of Bond Length (Å) and Bond Angle (deg) Data for ArSHgMe

Ar	$d(\text{Hg}-\text{C})/\text{\AA}$	$d(\text{Hg}-\text{S})/\text{\AA}$	$\text{C}-\text{Hg}-\text{S}/\text{deg}$	ref
$\text{C}_6\text{H}_5$	2.068(6)	2.383(2)	176.6(2)	
<i>o</i> - $\text{C}_6\text{H}_4\text{NO}_2$	2.08(2)	2.379(4)	176.4(5)	32f
	2.04(2)	2.366(4)	177.0(5)	
<i>m</i> - $\text{C}_6\text{H}_4\text{NH}_2$	2.074(14)	2.373(4)	175.5(5)	19a
	2.092(16)	2.379(4)	174.8(5)	
<i>m</i> - $\text{C}_6\text{H}_4\text{N}=\text{CHC}_6\text{H}_4\text{OH}$	2.071(12)	2.383(3)	178.7(4)	19a
	2.092(12)	2.379(3)	178.3(5)	
<i>p</i> - $\text{C}_6\text{H}_4\text{N}=\text{CHC}_6\text{H}_4\text{OH}$	2.05(4)	2.369(7)	176.5(11)	19a
	2.11(3)	2.384(8)	176.2(10)	

Evaluation of the data listed in Table 2 indicate that the coordination geometries about mercury in neutral PhSHgEt and anionic  $[(\text{ArCO}_2)\text{SHgEt}]^-$  are similar, such that the *ortho* carboxylate group does not significantly influence the Hg–Et bond length.

In contrast to mercury ethyl compounds of the type ArSHgEt, several mercury methyl counterparts have been structurally characterized, with the exception of the parent, PhSHgMe. Therefore, we have also determined the molecular structure of PhSHgMe (Figure 10). Consideration of the data in Table 4 indicates that the substituents, whether located in the *ortho*, *meta*, or *para* positions, has little impact on the mercury coordination geometry.

## Summary

In conclusion, single crystal X-ray diffraction studies demonstrate that, in the solid state, thimerosal consists of a complex network that features six crystallographically independent  $\{[(\text{ArCO}_2)\text{SHgEt}]\text{Na}\}$  formula units, each of which

possesses a similar coordination geometry at mercury.  $^1\text{H}$  NMR spectroscopic studies indicate that the appearance of the  $^{199}\text{Hg}$  mercury satellites of the ethyl group of thimerosal is highly dependent on the magnetic field and the viscosity of the solvent, an observation that is attributed to relaxation due to chemical shift anisotropy.

## Experimental Section

**General Considerations.** All manipulations were performed using a combination of glovebox, high-vacuum and Schlenk techniques under a nitrogen or argon atmosphere, except where otherwise stated. Solvents were purified and degassed by standard procedures. NMR spectra were measured on Bruker 300 DRX, Bruker 400 DRX and Bruker Avance 500 DMX spectrometers. For solutions in organic solvents,  $^1\text{H}$  NMR spectra are reported in ppm relative to  $\text{SiMe}_4$  ( $\delta = 0$ ) and were referenced internally with respect to the protio solvent impurity ( $\delta$  7.16 for  $\text{C}_6\text{D}_5\text{H}$ , 2.05 for  $(\text{CD}_3)_2\text{CO}$ , and 3.31 for  $\text{CD}_3\text{OD}$ ).<sup>36</sup> For aqueous solutions,  $^1\text{H}$  and  $^{13}\text{C}$  NMR chemical shift data are reported relative to the most upfield signal of internal sodium 3-(trimethylsilyl)-1-propanesulfonate, also known as sodium 2,2-dimethyl-2-silapentane-5-sulfonate, DSS ( $\delta_{\text{DSS}} = 0$ ).<sup>37</sup>  $^{199}\text{Hg}$  NMR chemical shifts are reported relative to  $\text{HgMe}_2$  ( $\delta = 0$ ) but in view of the toxicity of the latter compound, the spectra were referenced externally with respect to  $\text{HgI}_2$  (1 M in  $d_6$ -DMSO,  $\delta = -3106$ ).<sup>38</sup> Coupling constants are given in hertz. IR spectra were recorded as KBr pellets on a Nicolet Avatar DTGS spectrometer, and the data are reported in reciprocal centimeters. Thimerosal (Acros),  $\text{MeHgCl}$  (Aldrich),  $\text{EtHgCl}$  (Strem), and  $\text{PhSNa}$  (Fluka) were obtained commercially. Crystals of Thimerosal suitable for X-ray diffraction were obtained from methanol solution at room temperature.

**Caution!** All mercury compounds are toxic and appropriate safety precautions must be taken in handling these compounds.

**Spectroscopic Data for Thimerosal.**  $^1\text{H}$  NMR ( $\text{D}_2\text{O}$ ): 1.26 [t,  $^3J_{\text{H-H}} = 8$ ,  $^3J_{\text{H-Hg}} = 249$ , 3 H of  $\text{NaO}_2\text{CC}_6\text{H}_4\text{SHgCH}_2\text{CH}_3$ ], 1.65 [q,  $^3J_{\text{H-H}} = 8$ ,  $^3J_{\text{H-Hg}} = 173$ , 2 H of  $\text{NaO}_2\text{CC}_6\text{H}_4\text{SHgCH}_2\text{CH}_3$ ], 7.13–7.23 [m, 3H of  $\text{NaO}_2\text{CC}_6\text{H}_4\text{SHgCH}_2\text{CH}_3$ ], 7.49 [m, 1 H of  $\text{NaO}_2\text{CC}_6\text{H}_4\text{SHgCH}_2\text{CH}_3$ ].  $^1\text{H}$  NMR ( $\text{CD}_3\text{OD}$ ): 1.35 [t,  $^3J_{\text{H-H}} = 8$ ,  $^3J_{\text{H-Hg}} = 232$ , 3 H of  $\text{NaO}_2\text{CC}_6\text{H}_4\text{SHgCH}_2\text{CH}_3$ ], 1.65 [q,  $^3J_{\text{H-H}} = 8$ ,  $^3J_{\text{H-Hg}} = 173$ , 2 H of  $\text{NaO}_2\text{CC}_6\text{H}_4\text{SHgCH}_2\text{CH}_3$ ], 7.00–7.07 [m, 2 H of  $\text{NaO}_2\text{CC}_6\text{H}_4\text{SHgCH}_2\text{CH}_3$ ], 7.24 [m, 1H of  $\text{NaO}_2\text{CC}_6\text{H}_4\text{SHgCH}_2\text{CH}_3$ ], 7.41 [m, 1 H of  $\text{NaO}_2\text{CC}_6\text{H}_4\text{SHgCH}_2\text{CH}_3$ ].  $^1\text{H}$  NMR ( $(\text{CD}_3)_2$ -

(31) Viscosity of water = 0.890 cP; viscosity of methanol = 0.544 cP; viscosity of acetone = 0.306. See: *CRC Handbook of Chemistry and Physics*, 88th ed. (Internet Version 2008); Lide, D. R., Ed.; CRC Press/Taylor and Francis: Boca Raton, FL; pp 175–179.

(32) (a) Bach, R. D.; Weibel, A. T. *J. Am. Chem. Soc.* **1976**, *98*, 6241–6249. (b) Block, E.; Brito, M.; Gernon, M.; McGowty, D.; Kang, H.; Zubieta, J. *Inorg. Chem.* **1990**, *29*, 3172–3181. (c) Systma, L. F.; Kline, R. J. *J. Organomet. Chem.* **1973**, *54*, 15–21. (d) Sachs, G. *Ann. Chem.* **1923**, 433, 154–163. (e) Scheffold, R. *Helv. Chim. Acta* **1967**, *50*, 1419–1422. (f) Aupers, J. H.; Howie, R. A.; Wardell, J. L. *Polyhedron* **1997**, *16*, 2283–2289.

(33) Cambridge Structural Database (Version 5.28). 3D Search and Research Using the Cambridge Structural Database; Allen, F. H.; Kennard, O. *Chemical Design Automation News* **1993**, *8* (1), 31–37.

(34) PhSHgMe and PhSHgEt were obtained by the reaction of  $\text{RHgCl}$  ( $\text{R} = \text{Me}, \text{Et}$ ) with  $\text{NaSPh}$  (see Experimental Section), which is a slight modification of the general synthesis for  $\text{R'SHgR}$  involving the reaction of  $\text{RHgCl}$  with  $\text{NaOH}$  and  $\text{R'SH}$ . See reference 32a.

(35) For an early report of PhSHgEt, see reference 32d.

(36) Gottlieb, H. E.; Kotlyar, V.; Nudelman, A. *J. Org. Chem.* **1997**, *62*, 7512–7515.

(37) Harris, R. K.; Becker, E. D.; Cabral de Menezes, S. M.; Goodfellow, R.; Granger, P. *Pure Appl. Chem.* **2001**, *73*, 1795–1818.

(38) Kidd, R. G.; Goodfellow, R. J. In *NMR and the Periodic Table*; Harris, R. K., Mann, B. E., Eds.; Academic Press: New York, 1978; p 268.

CO): 1.29 [t,  $^3J_{\text{H-H}} = 8$ ,  $^3J_{\text{H-Hg}} = 230$ , 3 H of  $\text{NaO}_2\text{CC}_6\text{H}_4\text{SHg-CH}_2\text{CH}_3$ ], 1.47 [q,  $^3J_{\text{H-H}} = 8$ ,  $^3J_{\text{H-Hg}} = 173$ , 2 H of  $\text{NaO}_2\text{CC}_6\text{H}_4\text{SHgCH}_2\text{CH}_3$ ], 6.91–7.01 [m, 2 H of  $\text{NaO}_2\text{CC}_6\text{H}_4\text{SHgCH}_2\text{CH}_3$ ], 7.37–7.42 [m, 2 H of  $\text{NaO}_2\text{CC}_6\text{H}_4\text{SHgCH}_2\text{CH}_3$ ].  $^{13}\text{C}$  NMR ( $\text{D}_2\text{O}$ ): 15.9 [q,  $^1J_{\text{C-H}} = 126$ ,  $^2J_{\text{Hg-C}} = 74$ , 1 C of  $\text{NaO}_2\text{CC}_6\text{H}_4\text{SHgCH}_2\text{CH}_3$ ], 28.3 [t,  $^1J_{\text{C-H}} = 136$ ,  $^1J_{\text{Hg-C}} = 1316$ , 1 C of  $\text{NaO}_2\text{CC}_6\text{H}_4\text{SHgCH}_2\text{CH}_3$ ], 128.0 [d,  $^1J_{\text{C-H}} = 163$ , 1 C of  $\text{NaO}_2\text{CC}_6\text{H}_4\text{SHgCH}_2\text{CH}_3$ ], 128.2 [d,  $^1J_{\text{C-H}} = 163$ , 1 C of  $\text{NaO}_2\text{CC}_6\text{H}_4\text{SHgCH}_2\text{CH}_3$ ], 130.5 [d,  $^1J_{\text{C-H}} = 160$ , 1 C of  $\text{NaO}_2\text{CC}_6\text{H}_4\text{SHgCH}_2\text{CH}_3$ ], 132.5 [s, 1 C of  $\text{NaO}_2\text{CC}_6\text{H}_4\text{SHg-CH}_2\text{CH}_3$ ], 137.6 [d,  $^1J_{\text{C-H}} = 162$ , 1 C of  $\text{NaO}_2\text{CC}_6\text{H}_4\text{SHgCH}_2\text{CH}_3$ ], 147.0 [s, 1 C of  $\text{NaO}_2\text{CC}_6\text{H}_4\text{SHgCH}_2\text{CH}_3$ ], 181.4 [s, 1 C of  $\text{NaO}_2\text{CC}_6\text{H}_4\text{SHgCH}_2\text{CH}_3$ ]. IR Data (KBr,  $\text{cm}^{-1}$ ): 3042 (w), 2962 (w), 2917 (w), 2862 (w), 1610 (m), 1586 (s), 1569 (vs), 1547 (s), 1464 (w), 1454 (m), 1425 (m), 1410 (m), 1394 (s), 1387 (vs), 1373 (s), 1260 (m), 1246 (w), 1233 (w), 1177 (m), 1098 (br), 1054 (m), 1035 (m), 837 (m), 802 (m), 745 (s), 714 (m), 704 (m), 677 (m), 649 (m).  $^{199}\text{Hg}$  NMR ( $\text{D}_2\text{O}$ ): –784 [tq,  $^2J_{\text{Hg-H}} = 176$ ,  $^3J_{\text{Hg-H}} = 250$ ].

**Synthesis of PhSHgMe.** A mixture of PhSNa (211 mg, 1.60 mmol) and MeHgCl (400 mg, 1.59 mmol) was treated with  $\text{CH}_2\text{Cl}_2$  (20 mL), resulting in the immediate deposition of a white precipitate. The mixture was stirred for 2 h, allowed to settle for 30 min and filtered. The volatile components were removed in vacuo to give PhSHgMe as a white powder (325 mg, 63% yield). Crystals of composition PhSHgMe suitable for X-ray diffraction were obtained from  $\text{CH}_2\text{Cl}_2$ . Mass spectrum:  $m/z = 326.1$  [ $\text{M}^+$ ].  $^1\text{H}$  NMR ( $\text{C}_6\text{D}_6$ ): 0.19 [s,  $^2J_{\text{Hg-H}} = 163$ , PhSHg $\text{CH}_3$ ], 6.91 [t,  $^3J_{\text{H-H}} = 8$ ,  $p\text{-C}_6\text{H}_5\text{SHgMe}$ ], 7.00 [t,  $^3J_{\text{H-H}} = 8$ ,  $m\text{-C}_6\text{H}_5\text{SHgMe}$ ], 7.46 [d,  $^3J_{\text{H-H}} = 8$ ,  $o\text{-C}_6\text{H}_5\text{SHgMe}$ ]. IR Data (KBr pellet,  $\text{cm}^{-1}$ ): 3062 (w), 2991 (w), 2908 (w), 1578 (m), 1473 (vs), 1445 (w), 1432 (m), 1324 (w), 1265 (w), 1161 (w), 1084 (s), 1067 (m), 1023 (s), 886 (w), 775 (m), 730 (vs), 694 (m), 686 (s).

**Synthesis of PhSHgEt.** A mixture of PhSNa (150 mg, 1.14 mmol) and EtHgCl (301 mg, 1.14 mmol) was treated with  $\text{CH}_2\text{Cl}_2$  (25 mL), resulting in the immediate deposition of a white precipitate. The mixture was stirred for 2 h, allowed to settle for 30 min and filtered. The volatile components were removed in vacuo to give PhSHgEt as a white powder (260 mg, 68% yield). Crystals of composition PhSHgMe suitable for X-ray diffraction were obtained from  $\text{CH}_3\text{CN}$ . Mass spectrum:  $m/z = 340.1$  [ $\text{M}^+$ ].  $^1\text{H}$  NMR ( $\text{C}_6\text{D}_6$ ): 0.75 [t,  $^3J_{\text{H-H}} = 8$ ,  $^3J_{\text{H-Hg}} = 228$ , PhSHg $\text{CH}_2\text{CH}_3$ ], 0.95 [q,  $^3J_{\text{H-H}} = 8$ ,  $^3J_{\text{H-Hg}} = 162$ , PhSHg $\text{CH}_2\text{CH}_3$ ], 6.89 [t,  $^3J_{\text{H-H}} = 8$ ,  $p\text{-C}_6\text{H}_5\text{SHgEt}$ ], 6.97 [t,  $^3J_{\text{H-H}} = 8$ ,  $m\text{-C}_6\text{H}_5\text{SHgEt}$ ], 7.42 [d,  $^3J_{\text{H-H}} = 8$ ,  $o\text{-C}_6\text{H}_5\text{SHgEt}$ ]. IR Data (KBr pellet,  $\text{cm}^{-1}$ ): 3064 (w), 2965 (w), 2911 (w), 2856 (w), 1575 (m), 1473 (s), 1443 (w), 1433 (m), 1325 (w), 1229 (w), 1176 (w), 1161 (w), 1118 (w), 1083 (m), 1023 (m), 947 (w), 889 (w), 733 (vs), 692 (m), 687 (s), 677 (m).

**X-ray Structure Determinations.** Single crystal X-ray diffraction data were collected on either a Bruker Apex II diffractometer

**Table 5.** Crystal, Intensity Collection, and Refinement Data

	thimerosal	PhSHgMe	PhSHgEt
lattice	monoclinic	orthorhombic	monoclinic
formula	$\text{C}_9\text{H}_9\text{O}_2\text{SHgNa}$	$\text{C}_7\text{H}_8\text{HgS}$	$\text{C}_8\text{H}_{10}\text{HgS}$
formula weight	404.8	324.8	338.8
space group	$P2_1/c$	$Pbcn$	$Cc$
$a/\text{\AA}$	14.653(1)	23.863(1)	22.122(2)
$b/\text{\AA}$	25.455(2)	9.8304(5)	10.893(1)
$c/\text{\AA}$	17.730(1)	6.9604(4)	7.5251(8)
$\alpha/\text{deg}$	90	90	90
$\beta/\text{deg}$	103.418(1)	90	102.619(2)
$\gamma/\text{deg}$	90	90	90
$V/\text{\AA}^3$	6432.7(8)	1632.8(2)	1769.6(3)
$Z$	24	8	8
temperature (K)	125(2)	243(2)	243(2)
radiation ( $\lambda$ , $\text{\AA}$ )	0.71073	0.71073	0.71073
$\rho(\text{calcd.})$ , $\text{g cm}^{-3}$	2.508	2.642	2.543
$\mu(\text{Mo K}\alpha)$ , $\text{mm}^{-1}$	14.559	19.019	17.555
$\theta$ max, deg	31.69	28.34	28.27
no. of data collected	108850	10681	6174
no. of data used	21546	1971	2928
no. of parameters	758	83	183
$R_1$ [ $I > 2\sigma(I)$ ]	0.0611	0.0263	0.0272
$wR_2$ [ $I > 2\sigma(I)$ ]	0.1126	0.0523	0.0720
GOF	1.037	1.031	1.092

or a Bruker P4 diffractometer equipped with a SMART CCD detector. Crystal data, data collection, and refinement parameters are summarized in Table 5. The structures were solved using direct methods and standard difference map techniques and were refined by full-matrix least-squares procedures on  $F^2$  with SHELXTL (Versions 5.10 and 6.1).<sup>39</sup> Powder diffraction data for thimerosal were collected on a Bruker Apex II diffractometer, and the powder diffraction pattern based on the single crystal data was calculated with Mercury (Version 1.4.2).<sup>40</sup>

**Acknowledgment.** We thank the National Institutes of Health (GM046502) for support of this research. The National Science Foundation (CHE-0619638) is thanked for acquisition of an X-ray diffractometer.

**Supporting Information Available:** Experimental details, computational data, and crystallographic data in CIF format. This material is available free of charge via the Internet at <http://pubs.acs.org>.

IC8005426

- (39) (a) Sheldrick, G. M. *SHELXTL, An Integrated System for Solving, Refining and Displaying Crystal Structures from Diffraction Data*; University of Göttingen: Göttingen, Federal Republic of Germany, 1981. (b) Sheldrick, G. M. *Acta Crystallogr.* **2008**, A64, 112–122.
- (40) <http://www.ccdc.cam.ac.uk/mercury/>, May 2008.